Multimode bolometer development for the Primordial Inflation Explorer (PIXIE) instrument

Peter C. Nagler [1,2]

Kevin T. Crowley [3] Kevin L. Denis [1] Archana M. Devasia [1,4,5] Dale J. Fixsen [1,4]
Alan J. Kogut [1] George Manos [1] Scott Porter [1] Thomas R. Stevenson [1]

June 30, 2016

[1]NASA/GSFC
[2]Brown University
[3]Princeton University
[4]University of Maryland
[5]CRESST

Outline

1. Introduction and instrument description
2. Detector design and fabrication
3. Package and readout
4. Detector performance
5. Conclusions

Introduction and instrument description

Introduction

The Primordial Inflation Explorer (PIXIE) [1, 2]

- Space-based polarizing Fourier transform spectrometer (FTS).
- Designed to measure the polarization and intensity spectra of the CMB.
- Multimode "lightbucket" design enables nK-scale sensitivity across 2.5 decades in frequency with just 4 thermistor-based bolometers.
- Like other FTSs [3, 4, 5, 6], PIXIE's design and experimental approach[a] represent a significant departure from imagers often used for CMB measurements. *This is especially true for the detectors.*
  - Large etendue ($A\Omega = 4$ cm^2 sr).
  - Handle large optical load (120 pW).
  - Large and mechanically robust absorber structure (30x larger than the spider web bolometers on Planck [7]).
  - Limited sensitivity to particle hits.
  - Sensitive to all optical frequencies of interest (15 GHz - 5 THz).
  - Photon-noise limited (NEP $\leq 1 \times 10^{-16}$ $\mathrm{W}/\sqrt{\mathrm{Hz}}$).

[a] See Al Kogut's poster on systematic error mitigation and Dale Fixsen's talk on beams.

Instrument description

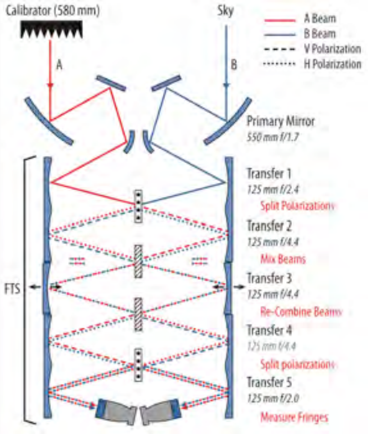

Each focal plane has two polarization-sensitive bolometers mounted back-to-back with their polarization axes orthogonal.

Incident radiation:

$$\vec{E}_{inc} = A\hat{x} + B\hat{y} \tag{1}$$

Measured power:

$$\begin{aligned}
\mathbf{P}_x^L &= \frac{1}{2}\int (A^2+B^2) + (A^2-B^2)\cos\left(\frac{4\nu z}{c}\right)d\nu. \\
\mathbf{P}_y^L &= \frac{1}{2}\int (A^2+B^2) + (B^2-A^2)\cos\left(\frac{4\nu z}{c}\right)d\nu. \\
\mathbf{P}_x^R &= \frac{1}{2}\int (A^2+B^2) + (A^2-B^2)\cos\left(\frac{4\nu z}{c}\right)d\nu. \\
\mathbf{P}_y^R &= \frac{1}{2}\int (A^2+B^2) + (B^2-A^2)\cos\left(\frac{4\nu z}{c}\right)d\nu.
\end{aligned} \tag{2}$$

Inverse Fourier transform:

$$\begin{aligned}
\mathbf{S}_x^L(\nu) &= A_\nu^2 - B_\nu^2. \\
\mathbf{S}_y^L(\nu) &= B_\nu^2 - A_\nu^2. \\
\mathbf{S}_x^R(\nu) &= A_\nu^2 - B_\nu^2. \\
\mathbf{S}_y^R(\nu) &= B_\nu^2 - A_\nu^2.
\end{aligned} \tag{3}$$

Signal = small modulated component in a bright $(\sim 120\,\mathrm{pW})$ *background.*

Instrument description

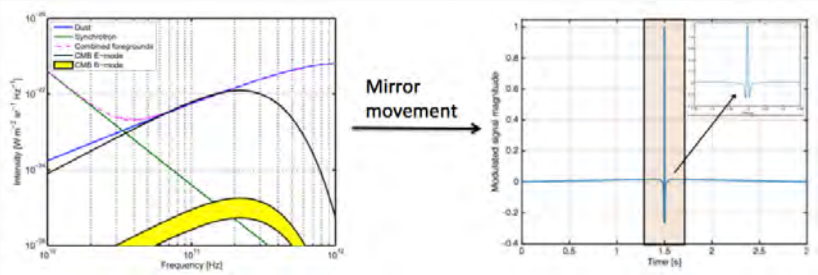

- Mirror position z $\rightarrow$ optical path difference ℓ: $z \simeq \ell/4$.
- Mirror velocity v: $v = z/\left(3\,\mathrm{sec}\right) = 1.73\,\mathrm{mm/sec}$.
- Optical path difference ℓ $\rightarrow$ interfering radio frequency ν: $\ell = c/\nu$.
- Radio frequency ν $\rightarrow$ Audio (FTS) frequency ω: $\omega = 4\nu v/c$.
- CMB: $\omega \lesssim 15$ Hz.
- Dust: $\omega \lesssim 100$ Hz.

These constraints drive the bolometer bias and bandwidth requirements. *Detectors must be photon noise limited across all FTS frequencies* $(0 - 100\,\mathrm{Hz})$ *under large, near-constant* $(\sim 120\,\mathrm{pW})$ *optical bias.*

Detector design and fabrication

Detector design - overview

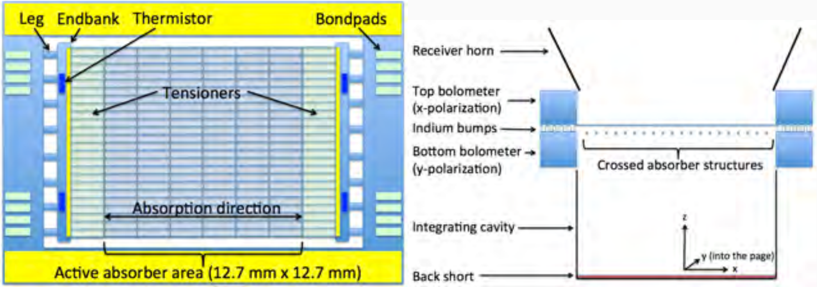

Detectors are fabricated using standard microfabrication techniques. They consist of three main components:

- Absorber structure - absorb single linear polarization
- Endbanks - measure incident optical power with silicon thermistors
- Frame - thermal sink and interface to readout

Each beam's focal plane will consist of two indium bump-hybridized detectors mounted $< 20\ \mu$m apart with their absorbers orthogonal.
$\rightarrow$ measure orthogonal polarizations of nearly the same electric field.

Absorber structure - overview

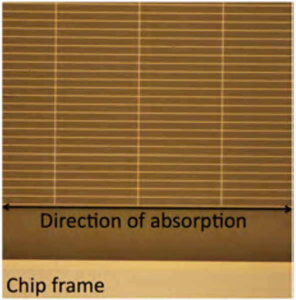

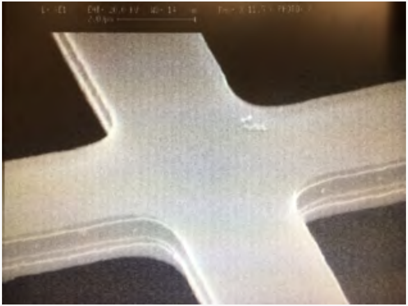

- Consists of a grid of suspended, micromachined, ion implanted silicon wires.
- Wires are degenerately doped to be metallic at all temperatures.
- Effective sheet resistance of the whole structure is 377 $\Omega/\square$.
- Absorber area sets low frequency cutoff of instrument (15 GHz); grid spacing (30 μm) sets high frequency cutoff (5 THz).
- Wire widths and thicknesses are highly uniform across the array.
    - Thickness set by starting SOI device layer thickness (1.35 μm).
    - Wires are etched to width with an ICP RIE process.

Absorber structure - mechanical characterization

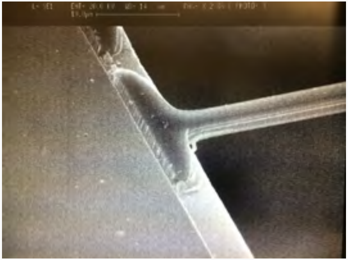

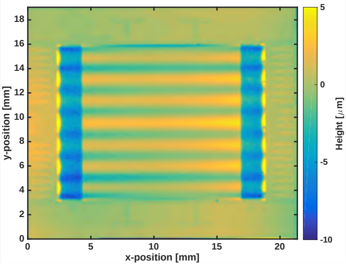

- Doping induces compressive stress in absorber wires; previous devices had their wires buckle and protrude up to 20 μm from the frame.
  $\rightarrow$ problematic for a hybridized pair of bolometers.
- Detectors subject to vibrations and acoustic excitations at launch.
  $\rightarrow$ need resonant frequencies of absorber structure to be much greater than excitation frequencies of launch.
- Solution: deposit highly tensile $\mathrm{Al_2O_3}$ film on absorbers outside of active optical region.
  $\rightarrow$ Fabricated absorbers are flat and expected to oscillate with amplitudes of < 0.4 μm rms during launch.

Endbanks - overview

- Consists of a gold bar for thermalization and two doped silicon thermistors on a crystalline silicon membrane.
- The gold bar also sets the heat capacity of the endbank.
- Endbank is formed from the device layer of the SOI substrate.

- Endbanks are connected to the chip frame through eight silicon legs.
- Thermistors are doped to operate below metal-insulator transition. Electron transport mechanism is variable range hopping [8]:

$$R(T) = R_0 \times \exp\sqrt{\frac{T_0}{T}}, \quad (4)$$

where R_0 and T_0 are constants largely determined by geometry and doping, respectively.

Frame

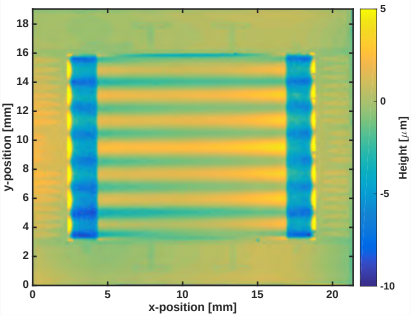

Figure 1: replace this with In bump SEM

- The chip frame is designed so that any two bolometer chips can be hybridized together.
- Large gold-covered areas serve as heat sinks.

Package and readout

Package and readout - dark tests

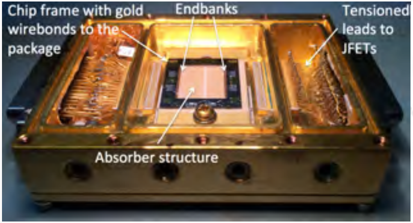

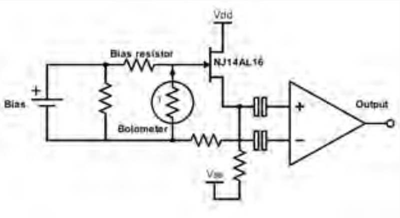

- Thermistor operates under current bias ($R_{bias} >> R_{therm}$).
- Bolometer is connected to a cryogenic (130 K) JFET amplifier with tensioned leads, mitigating capacitive microphonic contamination of the signal band. We use Interfet NJ14AL16 JFETs that are screened for low noise performance (5.5 $\mathrm{nV}/\sqrt{\mathrm{Hz}}$ at 100 Hz).
- Amplifier converts the high source impedance of the thermistors (MΩ-scale) to the low output impedance of the JFETs (1.8 kΩ).
- Low impedance signal is AC coupled to a room temperature amplifier.

Detector performance

Performance - load curves

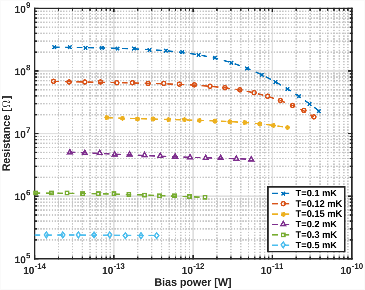

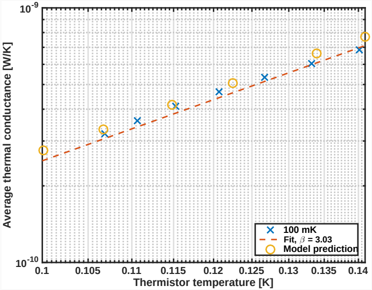

- Determine R_0 and T_0 from the measured resistances under low electrical bias.
  $\rightarrow$ $T_0 = 15.11$ K and $R_0 = 911\ \Omega$. Operating resistance: 5.42 MΩ.
- Determine average thermal conductance $\bar{G}$ between the thermistors and the bath from the high-bias end of the load curves:

$$\bar{G} = \frac{P_{\mathrm{bias}}}{T_1 - T_2}. \tag{5}$$

- Fit to the measured $\bar{G}$ with a function $\tilde{G} = G_0 \times T^{\beta}$.
  $\rightarrow$ The fit is close to the expected value ($\beta_{phonon} = 3$).

Performance - thermal model

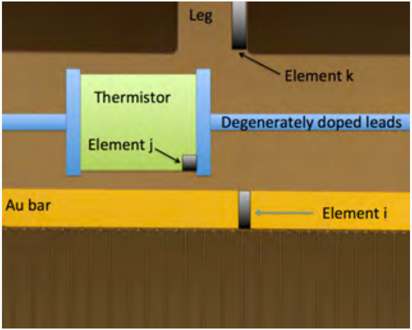

- For the endbank geometry, break Au bar, thermistors, and legs into small elements.
- Solve for the etendue $A\Omega_{ij,ik}$ beween all elements.
- Heat flow between elements (e.g., between i and j) is given by $P_{ij} = A_{ij}\left(T_i^{\nu} - T_j^{\nu}\right)$.

- Determine G between elements, determine C from material properties/geometries, measure VRH parameters R_0 and T_0, and solve for non-equilibrium bolometer noise [9]:

$$\mathrm{NEP_{bolometer}}^2 = \gamma_1 4 k_b T^2 G + \frac{1}{S^2}\left(\gamma_2 4 k_b T R + e_n^2 + \gamma_3 i_n^2 R + \gamma_4 \mathrm{NEP_{excess}}^2\right). \tag{6}$$

Performance - noise

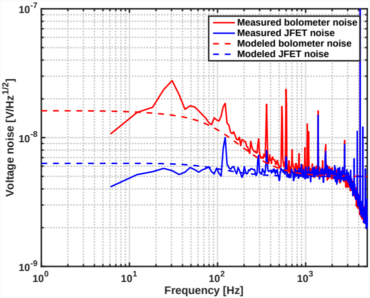

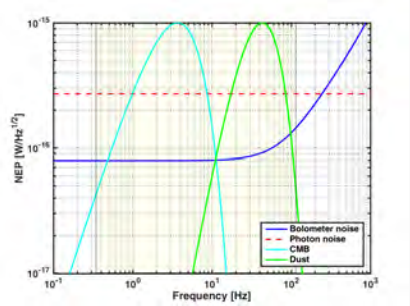

- Thermal model reproduces the measured $\bar{G}$ well.
- Modeled noise fits the measured noise well for multiple bias conditions.
- Running the model for the optical and electrical bias conditions expected during flight, we calculate a bolometer NEP of 7.93×10^{-17} W/$\sqrt{\mathrm{Hz}}$.

Expect to be photon noise limited across the entire PIXIE bandwidth.

Conclusions

Conclusions

- We designed, fabricated, and characterized large area polarization-sensitive bolometers for the PIXIE experiment.
- Mechanical characterization of the fabricated PIXIE bolometers shows that the tensioning scheme successfully flattens the absorber strings.
    - Enables indium bump hybridization of a pair of bolometer chips.
    - Mitigates microphonic sensitivity during launch.
- The dark data provide significant insight into the thermal behavior of the endbanks.
    - Thermal model agress well with the data.
    - The results indicate that the PIXIE bolometers satisfy the sensitivity and bandwidth requirements of the space mission.
- Upcoming work:
    - Characterize the absorber structure (dark measurements of thermal transport and AC impedance, optical measurements with a cryogenic blackbody source.)
    - Subject a hybridized pair of bolometers to environmental testing.

Acknowledgements

This work was supported by NASA/GSFC IRAD funding. We are especially grateful to the x-ray microcalorimeter group at NASA/GSFC for lending the Astro-E2/Suzaku test platform for PIXIE detector characterization.

Backup

Backup

References I

- A. Kogut, D. J. Fixsen, D. T. Chuss, J. Dotson, E. Dwek, M. Halpern, G. F. Hinshaw, S. M. Meyer, S. H. Moseley, M. D. Seiffert, D. N. Spergel, and E. J. Wollack, "The Primordial Inflation Explorer (PIXIE): a nulling polarimeter for cosmic microwave background observations," *JCAP* **7**, p. 025, July 2011.
- A. Kogut, D. T. Chuss, J. Dotson, E. Dwek, D. J. Fixsen, M. Halpern, G. F. Hinshaw, S. Meyer, S. H. Moseley, M. D. Seiffert, D. N. Spergel, and E. J. Wollack, "The Primordial Inflation Explorer (PIXIE)," in *Space Telescopes and Instrumentation 2014: Optical, Infrared, and Millimeter Wave*, *Proc. SPIE* **9143**, p. 91431E, Aug. 2014.
- D. P. Woody and P. L. Richards, "Near-millimeter spectrum of the microwave background," *ApJ* **248**, pp. 18–37, Aug. 1981.

References II

- H. P. Gush, M. Halpern, and E. H. Wishnow, "Rocket measurement of the cosmic-background-radiation mm-wave spectrum," *Physical Review Letters* **65**, pp. 537–540, July 1990.
- J. C. Mather, E. S. Cheng, D. A. Cottingham, R. E. Eplee, Jr., D. J. Fixsen, T. Hewagama, R. B. Isaacman, K. A. Jensen, S. S. Meyer, P. D. Noerdlinger, S. M. Read, L. P. Rosen, R. A. Shafer, E. L. Wright, C. L. Bennett, N. W. Boggess, M. G. Hauser, T. Kelsall, S. H. Moseley, Jr., R. F. Silverberg, G. F. Smoot, R. Weiss, and D. T. Wilkinson, "Measurement of the cosmic microwave background spectrum by the COBE FIRAS instrument," *ApJ* **420**, pp. 439–444, Jan. 1994.

References III

- G. S. Tucker, H. P. Gush, M. Halpern, I. Shinkoda, and W. Towlson, "Anisotropy in the Microwave Sky: Results from the First Flight of the Balloon-borne Anisotropy Measurement (BAM)," *ApJ* **475**, pp. L73–L76, Feb. 1997.
- W. A. Holmes, J. J. Bock, B. P. Crill, T. C. Koch, W. C. Jones, A. E. Lange, and C. G. Paine, "Initial test results on bolometers for the Planck high frequency instrument," *Applied Optics* **47**, pp. 5996–6008, Nov. 2008.
- B. I. Shklovskii and A. L. Efros, *Electronic properties of doped semiconductors*, vol. 45, Springer Science & Business Media, 2013.
- J. C. Mather, "Bolometer noise: nonequilibrium thoery," *Applied Optics* **21**, pp. 1125–1129, Mar. 1982.